



10th World Conference on Neutron Radiography 5-10 October 2014

The influence of the heating condition on the void fraction in a boiling channel

H.Umekawa^{a*}, S.Nakamura^a, S.Fujiyoshi^a, T.Ami^a, M.Ozawa^a, Y.Saito^b and D.Ito^b

^aKansai University, Yamatecho, 3-3-35, Suita Osaka 564-8680, Japan

^bKyoto University Research Reactor Institute, Asashiro-nishi 2, Kumatori-cho, Sennan-gun, Osaka 590-0494, Japan

Abstract

The void fraction profile in a boiling channel is essential in analyzing convective flow boiling, where several investigations have been conducted. But due to the difficulty in the treatment of the non-thermodynamic equilibrium phenomena under subcooled conditions, the issues in comprehensive void fraction profile has not been solved, yet. To improve the understanding of these phenomena, detailed measurement results are required. In this investigation, by using five kinds of test sections, i.e. I.D.=3 mm L=400 mm, I.D.=5 mm L=200, 400, 1000 mm, and I.D.=10 mm L=400 mm, the void fraction was measured quantitatively over the whole length. For the measurements, thermal neutron radiography at the B-4 port of the Kyoto University Research Reactor was used. This facility is designed for the visualization of forced convective flow boiling in vertical tubes. To introduce the performance of this facility, this paper presents the measurement results of void fraction and the estimation results briefly.

© 2015 The Authors. Published by Elsevier B.V. This is an open access article under the CC BY-NC-ND license (<http://creativecommons.org/licenses/by-nc-nd/4.0/>).

Selection and peer-review under responsibility of Paul Scherrer Institut

Keywords; Void fraction, Two-phase flow, Net vapor generation, Convective flow boiling, Neutron radiography

1. Introduction

The void fraction profile in the boiling channel is very important in understanding the two-phase flow. This is because the void fraction includes the key information of the two-phase flow, such as the relationship between the liquid and vapor velocities even in the case of the simple one-dimensional treatment. Thus far numerous

* Corresponding author. Tel.: +81-6-6368-0807; fax: +81-6-6368-0807.

E-mail address: umekawa@kansai-u.ac.jp

investigations have been conducted (eg. Rouhani(1970), Sekoguchi(1980)). But due to the difficulty in the treatment of the non-thermodynamic equilibrium phenomena under subcooled condition, this classical problem of void fraction characteristics has not been fully understood (Ahmadi(2012), Kurul(1990)).

The general characteristics of void fraction of subcooled boiling can be found in several literatures. (eg. Sekoguchi(1973), Ueda(1989), Collier(1994), Tong(1997), Kandlikar(1999), Ozawa(2006)). As shown in Fig.1, for example, with the increase in the thermodynamic equilibrium quality of the inlet water by heating, the nucleation occurs at a certain point, i.e. Onset of Nucleate Boiling (ONB) under subcooled condition. Even after ONB, the void fraction still maintains a low level called as the wall voidage, but finally increases drastically. This point is recognized as Fully Developed Boiling or the Point of Net Vapor Generation (PNVG). Beyond PNVG, the void fraction increases under non-thermodynamic equilibrium condition, and finally achieves a thermodynamic equilibrium condition. This characteristic is widely known, however the actual phenomena are not as simple as those written in the literature. Moreover, due to the increase in the heat flux of present industrial equipment, a more accurate understanding of the subcooled boiling is required. The difficulty of the treatment of ONB comes from the difficulty of the treatment of the nucleation itself, thus a similar problem with pool boiling must be considered. In the case of the PNVG, the bubble behavior after nucleation, which includes the phase change caused by the contact with the subcooling water, must be treated. Of course, several trials have been presented theoretically and experimentally, but these void fraction characteristics are strongly influenced by many parameters, i.e. the magnitude of the heat flux, mass flux, degrees of the subcooling, geometry of the boiling channel, liquid properties and surface condition of heater. In this regard, several accurate experimental data are still required, where B-4 ports in KUR is considered as the suitable facility. In this report, actual quantitative measurements data and estimation results will be briefly presented.

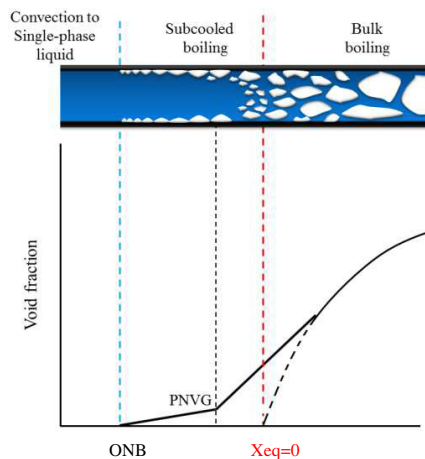


Fig.1 Void fraction in subcooled Boiling

2. Experiment

2.1. Experimental apparatus

The experimental apparatus was a forced convective boiling loop with a vertical heating tube, and degassed-ion-exchanged water was used as the working fluid. The setup mainly consisted of a control unit for the inlet water condition, a flow meter, a test section and a separator (Fig. 1(a)). The control unit had a condenser, a reserve tank, a preheater and a pump. By using this unit, during the experiment, the inlet water temperature was kept to 80 °C. The water controlled by this unit was sent to the test section, and heated by the direct Joule heating of D.C. power (max 20 V, 1200 A). Two-phase-mixture generated in the test section was sent to the separator and back to the

reserve tank through the condenser. In this investigation, five kinds of stainless tubes were used as the test section. The dimensions of each tube are listed in Table 1 together with the experimental conditions. While the experiment was conducted the measurement for the wall temperature, water temperatures at the inlet and outlet, the absolute pressure at the tube exit, the pressure difference over the test section, and the flow rate were also recorded.

Table 1. Dimensions of test sections and experimental conditions

I.D. (mm)	5.0	5.0	5.0	3.0	10.0
O.D. (mm)	7.0	7.0	7.0	5.0	11.0
Heating length L (mm)	200	400	1000	400	400
Heat flux q (kW/m ²)	810-2441	198-1700	168-497	198-604	421-1233
System pressure P (MPa)	0.3-0.5	0.3-0.8	0.3-0.8	0.3-0.6	0.3-1.1
Mass flux G (kg/m ² s)	600	300,450,600,1000	600	1000	300

For the quantitative measurement by thermal neutron radiography, the B-4 port of the Kyoto University Research Reactor was used, as shown in Fig.1(b). The thermal neutron flux at the exit of the B-4 port is 10^7 n/(cm²s). The beam size was approximately 10 mm in width and 80 mm in height at the exit of the port and 40 mm in width and 125 mm in height at the converter. The distance between the beam port exit and converter was 4.7 m. As the neutron converter, a ZNSL-L100-AL1016 (Chichibu Fuji co.) scintillation screen was used and 68 mm in height and 41 mm in width could be visualized. Images were taken by a C-CCD camera (PIXIS 1024B, Princeton Instruments). Although the visualization area of this facility is relatively small, the whole of the test section can be visualized by using the elevating frame which is built in the pit hole. This facility also has low voltage and high current D.C. power supply for the direct heating of the tubes and a water control unit as mentioned before. Therefore, this facility is considered as suitable for visualizing the boiling two-phase flow.

2.2. Image processing

Images were taken by a C-CCD camera as 16 bits data, with the pixel size corresponding to 0.067 mm/pixel. The exposure time was 20 seconds for 3.0 mm and 5.0 mm tubes, and 30 seconds for the 10 mm tube. For the quantitative estimation, 4 images, i.e. an offset image O , a single liquid phase image S_L , a tube image S_G and a two-phase image S_{TP} were taken, and the void fraction α is calculated by using Eq.(1). Before the calculation, to remove the white spot noise, a Morphology filter (Motomura (1996)) was also used as pre-processing.

$$\begin{aligned}
 S_{G(x,z,t)} &= G_{(x,z,t)} \exp(-\rho_w \mu_{mw} \delta_{w(x,z)}) + O_{(x,z,t)} \\
 S_{L(x,z,t)} &= G_{(x,z,t)} \exp(-\rho_L \mu_{mL} \delta_{L(x,z)} - \rho_w \mu_{mw} \delta_{w(x,z)}) + O_{(x,z,t)} \\
 S_{TP(x,z,t)} &= G_{(x,z,t)} \exp(-\rho_L \mu_{mL} \delta_{L(x,z)} (1 - \alpha_{(x,z,t)}) - \rho_w \mu_{mw} \delta_{w(x,z)}) + O_{(x,z,t)} \\
 \alpha_{(x,z)} &= \frac{\ln(S_{TP(x,z)} - O_{(x,z)}) - \ln(S_{L(x,z)} - O_{(x,z)})}{\ln(S_{G(x,z)} - O_{(x,z)}) - \ln(S_{L(x,z)} - O_{(x,z)})} \quad (1)
 \end{aligned}$$

where, G is gain, ρ is density, μ_m is mass attenuation coefficient, δ is thickness. Subscript G, L, TP, and W mean gas phase, liquid phase, two-phase and wall of test section, respectively.

Firstly, the influence of several factors on the accuracy of the quantitative measurement will be briefly explained.

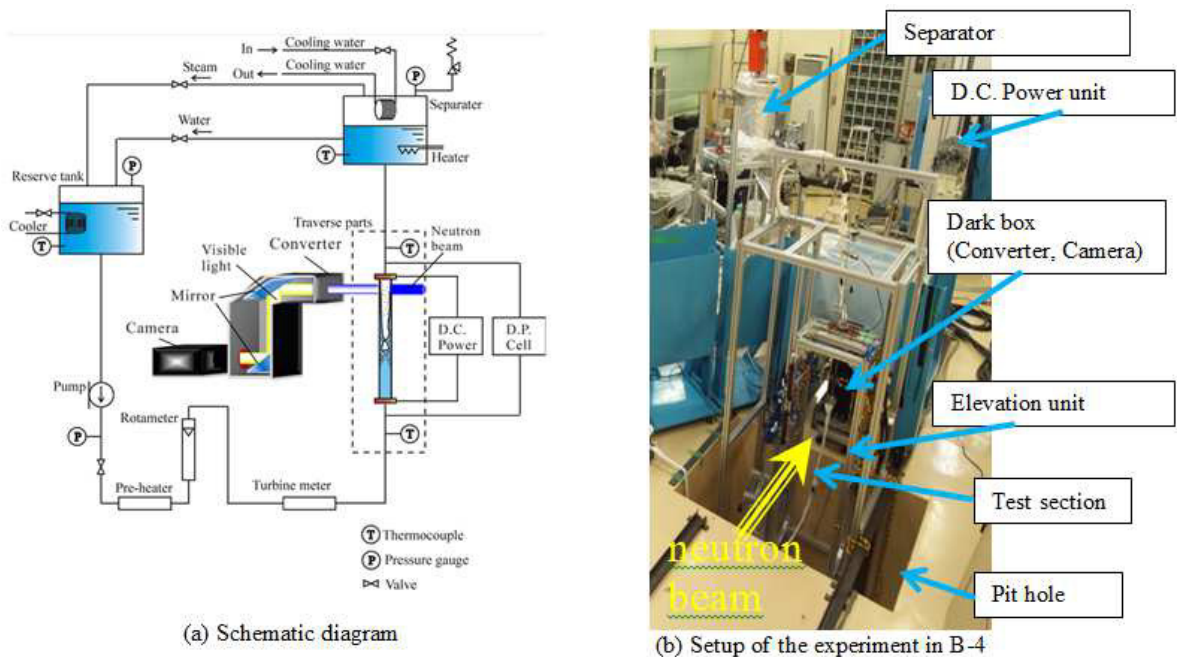


Fig.2 Experimental apparatus

- Stability of the offset and gain

On the basis of the actual measuring results, fluctuation of offset was less than 5 as gray-level, and this value corresponded to less than 0.1 percent of dynamic range.

The maximum fluctuation of the gain was less than 25, which corresponded to 0.015 in void fraction. In this stage, these values could be considered as negligible.

- Blurring of the beam

In this investigation long distance existed between the beam exit and object. Thus, blurring of the beam has been estimated by using the beam size at the beam exit and at the converter. On the basis of the geometrical relationship, the blurring has been estimated as 0.1 mm in vertical direction and 0.8mm in horizontal direction. In the estimation, the spatial moving average was used by the blurring size.

- Dynamic range

Measuring results of dynamic ranges became 1800 for 3 mm tube, 2100 for 5 mm tube and 4400 for 10 mm tube. These values mean this method can measure the 0.01 mm thickness water if 10 percent error is acceptable.

- Scattering

For compensating the scattering, three methods, i.e. Umbra, Greodel and Collimator methods, are known (Takenaka(2001)). In this paper, the influence of the scattering was estimated by using the Umbra method. For the estimation, 5 mm width grid spacer made of B₄C was used. Although the maximum error reached 20 percent in the case of low void fraction(less than 0.05), the magnitude of the deviation itself was not so large. In this case the distance between the test section and converter was about 30mm, with which the Greodel method can be applied.

On the basis of these estimations, the spatial resolution of these measurements were estimated as 0.1 mm in the width and 0.8 mm in the height, the time resolution was 30s, and the accuracy of the void fraction is ± 0.01 .

2.3. Measurement results

Figure 3(a) shows a 2-dimensional void fraction image which is constructed by using the successive eight images, and the color corresponds to the void fraction indicated by the color scale. In the figure, z , p , G , T_{in} , and q correspond to the distance from the tube inlet, pressure, mass flux, inlet temperature and heat flux, respectively.

Void fraction α in this figure corresponds to the mean ratio along the beam pass, but even in this expression, void fraction characteristics along the horizontal direction can be observed clearly. For example the wall voidage under subcooled condition at the inlet side, and center high voidage in annular flow regime at the exit side are quite well visualized. Also the start of the center voidage in Fig. 3(a) is in good agreement with the Mishima's flow regime transition condition between the bubbly flow and slug flow which is drawn in Fig. 3(b).

The longitudinal void fraction profile which corresponds to the center axis data of Fig. 3(a) is plotted against the distance from the inlet z in Fig. 3(b). At three elevations which are pointed by arrows, i.e. $z=150, 210, 370$ mm, the void fraction along the horizontal direction are also plotted in Fig. 3(c), and the radial direction profile which is calculated by using Abel transformation with the assumption of axial symmetry is plotted in Fig.3(d). As shown in Fig.3(c) and (d), the evaluation procedure strongly influences the magnitude of the obtained void fraction, especially the value at the center. Thus, for a detailed discussion, this must be considered carefully. Here only the general feature will be introduced.

In Fig.3(b) the net-vapor generation point estimated by Saha-Zuber(1974) is also plotted by a dashed line. Apparently the localization of the net vapor generation point itself is not clear, but the drastic increase of the void fraction occurred at the lower quality side when compared with the estimation results. In the figure, several correlations (e.g. Ozawa(2013)) are also drawn. Although these correlations show good agreements with data qualitatively, large deviations can be observed quantitatively.

In the void fraction profile at the position of 150 mm Fig.3(d), the wall peak characteristics can be clearly observed. To understand the characteristics of subcooled boiling, the estimation of the propagation of this wall voidage becomes very important. To achieve this requirement, the void fraction profile on the basis of the shadow image is not enough, and the profile along the radial direction must be obtained. It may require a more precise measurement to achieve the axial symmetry assumption. Nevertheless the data show the possibility of the estimation of subcooled boiling by using neutron radiography.

In Fig.4, void fraction data under several conditions are plotted. In this figure, the data are plotted against the thermodynamic equilibrium quality x_{eq} , and several correlations which were used in Fig.3(b) are also drawn. In these figures the net vapor generation point estimated by the Saha-Zuber is shown with arrows. The Peclet number of this investigation becomes lower than 700,000. Thus, on the basis of Saha-Zuber's model, this region is controlled by the thermodynamic condition, but the deviation means a weaker restriction of the thermodynamic condition. Including these characteristics, a detailed discussion will be published elsewhere.

Also as shown in Fig.4, correlations take a relatively similar tendency compared to each other under low heat flux condition, while under high heat flux condition each evaluation scatters widely. To discuss more exhaustive comparison, especially about the ONB and PNVG conditions, more details on the evaluation of the experimental condition must be included, especially the compensation of the pressure drop. Thus, in this paper only the remarkable characteristics are introduced. After PNVG, the increasing rate of the void fraction $d\alpha/dx_{eq}$ will also express the speed of the relaxation of the non-thermodynamic equilibrium condition. In Fig.5(a), to confirm this characteristic, $d\alpha/dx_{eq}$ is plotted against the heat flux. Even under first rough estimation, the data demonstrate the influence of the heat flux and the influence of the tube diameter. In Fig.5(b), the same data are weighted by using the tube diameter ratio, and the results are in good agreement in this condition. The void fraction data among a whole of the test section can be quantitatively obtained in this apparatus, and these data are very useful in the wide range of discussion.

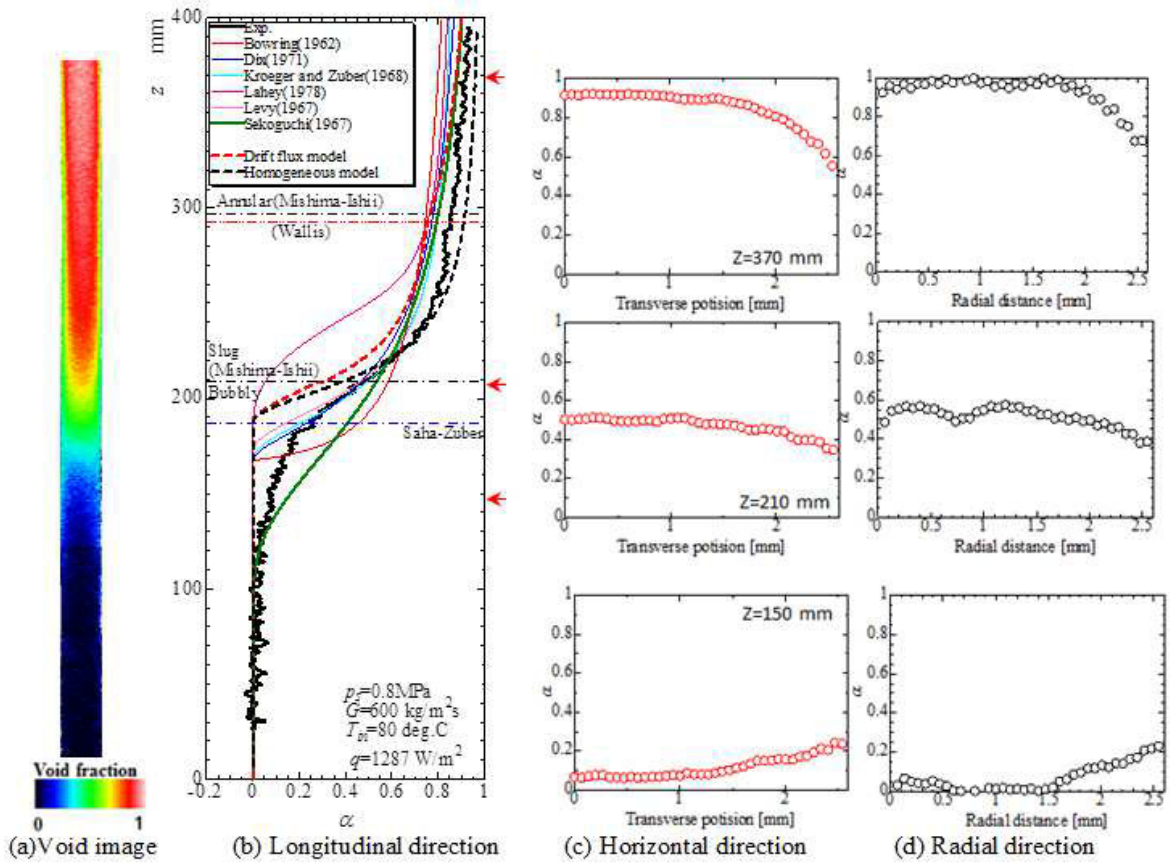


Fig.3 Measurement results of Void fraction

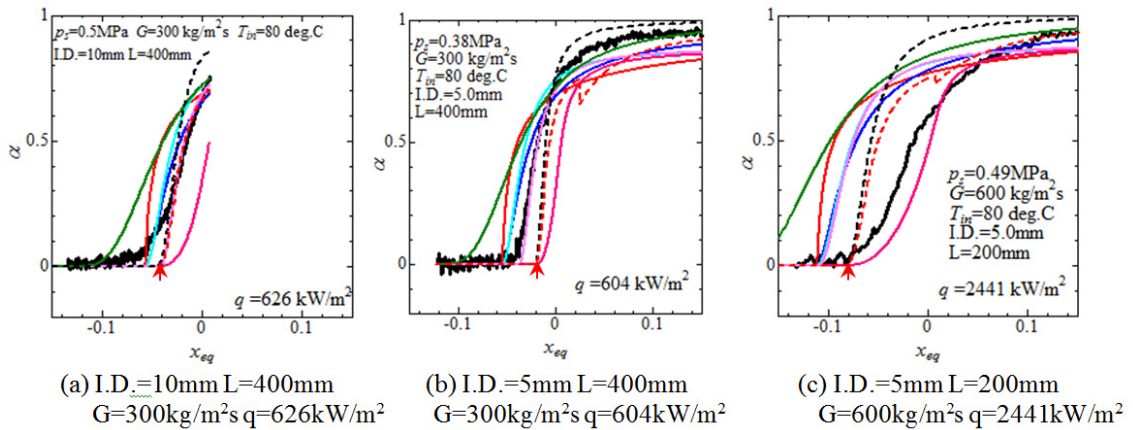


Fig.4 Comparison of the Heating condition

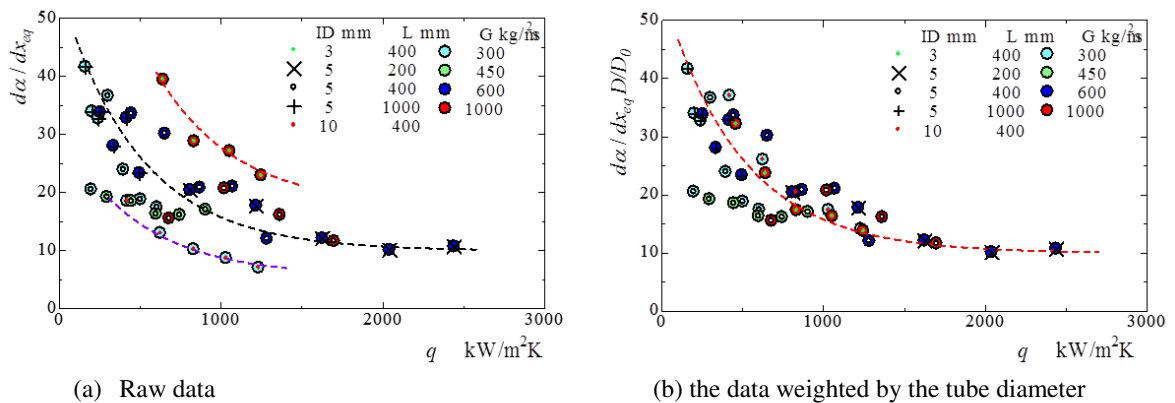


Fig.5 The increasing tendency of the void fraction against the thermodynamic equilibrium quality

3. Summary

This paper explained the measurement of the void fraction in a boiling channel, and also introduced the performance of the B-4 port of KUR as a specialized facility for the visualization of the boiling channel. On the basis of the measuring results, a simple evaluation of the void fraction profile was explained briefly.

These results mean that the measured data has enough quality and are also very useful in improving the understanding of subcooled boiling.

Acknowledgements

The authors wish to express their sincere thanks to Prof. Takenaka, N. for his technical support. They also would like to thank Mr. Sakakura, K., Mr. Yamashina, G., Mr. Harada, T., Mr. Nakano, R. for their support during the experiment. This investigation was carried out in part under the Visiting Researcher's Program of the Research Reactor Institute of Kyoto University (23P12-5, 24P4-5)

Reference

- Ahmadi, R., Ueno, T. and Okawa, T., 2012. Experimental Identification of the Phenomenon Triggering the Net Vapor Generation in Upward Subcooled Flow Boiling of Water at Low Pressure. *Int. J. Heat and Mass Transf.* 55, 6067-6076.
- Bowring, R.W., 1962. Physical Model Based on Bubble Detachment and Calculation of Steam Voidage in the Subcooled Region of a Heated Channel. Rep.HOR-10, Institute for Atomenergi.
- Collier, J.G. and Thome, J.R., 1994. *Convective Boiling and Condensation* 3rd edition. Clarendon Press, Oxford, 220-248.
- Kandlikar, S.G. and Nariyai, H., 1999. *Handbook of Phase Change: Boiling and Condensation* (S.G.Kandlikar, M.Shoji and V.K.Dhir eds.). Taylor and Francis, 368-386.
- Kurul, N. and Podowski, M.Z., 1990. Multidimensional Effects in Forced Convection Subcooled Boiling. *Proc. 9th Int. Heat Transf. Conf.*, 21-26.
- Motomura, Y., Ono, A. and Takenaka, N., 1996. Suppression of Isolated Noise in the Dynamic Neutron Radiography Image by Use of Mathematical Morphology. *Nuclear Instruments and Method in Physics research A*, 377, 93-95.
- Ozawa, M., 2006. *Handbook of Gas-Liquid Two-phase Flow Technology* 2nd edition (in Japanese)(JSME eds.). Korona, 51-62.
- Ozawa, M. and Ami, T., 2013. *Design Handbook of Boiling Two-Phase Flow*. Technosystem, 44-59.
- Rouhani, S.Z. and Axelsson, E., 1970. Calculation of Void Volume Fraction in the Subcooled and Quality Boiling Regions. *Int. J. Heat Mass Transfer*, Vol.13, pp.383-393.
- Saha, P. and Zuber, N., 1974. Point of Net Vapor Generation and Vapor Void Fraction in Subcooled Boiling. *Proc. 5th Int. Heat Transfer Conf.* 4, 175-179.
- Sekoguchi, K., 1973. *Advances in Heattransfer* (in Japanese), 217-233.
- Sekoguchi, K., Tanaka, O., Esaki, S. and Imasaka, T., 1980. Estimation Method of Void Fraction under Low Quality Region in Boiling Flow. 46(401), 111-120.

- Takenaka, N., 2001, Radiography for Visualization and Measurement of Gas-liquid Two-phase Flow, J. Visualization Society Japan, 21-80,14-20.
- Tong, L.S. and Tang, Y.S.,1997. Boiling Heat Transfer and Two-Phase Flow 2nd edition, Taylor& Francis, 152-155.
- Ueda, T., 1989. Gas-liquid Two-Phase Flow- Flow and Heat transfer-(in Japanese), Youken-do.243-255.